ORIGINAL ARTICLE

JBMR

# Conditional Deletion of *Bmpr1a* in Differentiated Osteoclasts Increases Osteoblastic Bone Formation, Increasing Volume of Remodeling Bone in Mice

Mina Okamoto,[1,2,3] Junko Murai,[1,2] Yuuki Imai,[4] Daisuke Ikegami,[1,2] Nobuhiro Kamiya,[5] Shigeaki Kato,[4] Yuji Mishina,[6] Hideki Yoshikawa,[2] and Noriyuki Tsumaki[1,2,3,7]

[1]Department of Bone and Cartilage Biology, Osaka University Graduate School of Medicine, Osaka, Japan
[2]Department of Orthopaedic Surgery, Osaka University Graduate School of Medicine, Osaka, Japan
[3]Japan Science and Technology Agency, Tokyo, Japan
[4]Institute of Molecular and Cellular Biosciences, University of Tokyo, Tokyo, Japan
[5]Center for Excellence in Hip Disorders, Texas Scottish Rite Hospital for Children, Dallas, TX, USA
[6]School of Dentistry, University of Michigan, Ann Arbor, MI, USA
[7]Center for iPS Cell Research and Application, Kyoto University, Kyoto, Japan

**ABSTRACT**

Bone undergoes remodeling consisting of osteoclastic bone resorption followed by osteoblastic bone formation throughout life. Although the effects of bone morphogenetic protein (BMP) signals on osteoblasts have been studied extensively, the function of BMP signals in osteoclasts has not been fully elucidated. To delineate the function of BMP signals in osteoclasts during bone remodeling, we deleted *BMP receptor type IA* (*Bmpr1a*) in an osteoclast-specific manner using a knock-in Cre mouse line to the *cathepsin K* locus ($Ctsk^{Cre/+}$; $Bmpr1a^{flox/flox}$, designated as $Bmpr1a^{\Delta Oc/\Delta Oc}$). Cre was specifically expressed in multinucleated osteoclasts in vivo. Cre-dependent deletion of the *Bmpr1a* gene occurred at 4 days after cultivation of bone marrow macrophages obtained from $Bmpr1a^{\Delta Oc/\Delta Oc}$ with RANKL. These results suggested that *Bmpr1a* was deleted after formation of osteoclasts in $Bmpr1a^{\Delta Oc/\Delta Oc}$ mice. Expression of bone-resorption markers increased, thus suggesting that BMPRIA signaling negatively regulates osteoclast differentiation. Trabeculae in tibia and femurs were thickened in 3.5-, 8-, and 12-week-old $Bmpr1a^{\Delta Oc/\Delta Oc}$ mice. Bone histomorphometry revealed increased bone volume associated with increased osteoblastic bone-formation rates (BFR) in the remodeling bone of the secondary spongiosa in $Bmpr1a^{\Delta Oc/\Delta Oc}$ tibias at 8 weeks of age. For comparison, we also induced an osteoblast-specific deletion of *Bmpr1a* using *Col1a1-Cre*. The resulting mice showed increased bone volume with marked decreases in BFR in tibias at 8 weeks of age. These results indicate that deletion of *Bmpr1a* in differentiated osteoclasts increases osteoblastic bone formation, thus suggesting that BMPR1A signaling in osteoclasts regulates coupling to osteoblasts by reducing bone-formation activity during bone remodeling. © 2011 American Society for Bone and Mineral Research.

**KEY WORDS:** BONE MORPHOGENETIC PROTEIN RECEPTOR TYPE IA; CATHEPSIN K; OSTEOCLASTS; OSTEOBLASTS; COUPLING

## Introduction

Bone is formed by replacing cartilage during endochondoral bone formation. Osteoblasts carried by blood vessels form woven bone on the remnants of the calcified cartilage matrix, modeling the trabeculae of the primary spongiosa. The primary spongiosa then undergoes remodeling consisting of bone resorption followed by bone formation, creating secondary spongiosa. This bone remodeling continues during bone growth and homeostasis throughout life.[1] At the initiation phase of bone remodeling, hematopoietic precursors are recruited to the surface of trabecular bone. The precursors respond to RANKL produced by osteoblasts and stromal cells and differentiate into osteoclasts,[2] which dominate bone resorption. Subsequently, the transition from bone resorption to bone formation is considered to be mediated by osteoclast-derived coupling factors. Coupling factors may include factors released from bone matrix after resorption by osteoclasts and factors produced by

Received in original form November 9, 2010; revised form April 28, 2011; accepted June 20, 2011. Published online July 22, 2011.
Address correspondence to: Noriyuki Tsumaki, MD, PhD, Center for iPS Cell Research and Application, Kyoto University, 53 Kawahara-cho, Shogoin, Sakyo-ku, Kyoto 606-8507, Japan. E-mail: ntsumaki@cira.kyoto-u.ac.jp
Additional Supporting Information may be found in the online version of this article.

Journal of Bone and Mineral Research, Vol. 26, No. 10, October 2011, pp 2511–2522
DOI: 10.1002/jbmr.477

osteoclasts. Transforming growth factor β (TGF-β) released from bone matrix has been shown to stimulate bone formation.[3,4] Osteoclasts have been shown to regulate osteoblast differentiation by producing ephrinB2.[5] Although several molecules are considered to be coupling factors,[6] the in vivo phenomenon of regulating osteoblast differentiation by osteoclasts remains to be documented.

Bone morphogenetic proteins (BMPs) were identified initially as secreted substances capable of inducing ectopic formation of cartilage and bone when implanted subcutaneously or in muscle pouches.[7] Subsequent molecular cloning studies have revealed that BMPs comprise a large subfamily of the TGF-β superfamily.[8] BMPs bind to BMP receptor types 1 and 2, and their signals are mediated by phosphorylation of receptor-regulated Smads (R-Smads), such as Smads 1, 5, and 8.[9] Phosphorylated R-Smads form heteromers with Smad 4, which is a common-partner Smad (Co-Smad), and the heteromers translocate into the nucleus.

Extensive studies have characterized BMPs as inducing factors of osteoblastic bone formation. Osteoblast-specific downregulation of BMP signals in mice has clarified the role of BMPs in osteoblast differentiation. In 4-week-old to 6-month-old mice, osteoblast-specific expression of dominant-negative BMP receptor type 1B[10] and mature osteoblast-specific gene ablation of BMP receptor type 1A (BMPR1A) mediated by the osteocalcin promoter–*Cre* transgene[11] causes inhibition of osteoblast differentiation and a decrease in bone volume, indicating that BMP signals are important for maintenance of bone mass by osteoblasts.

With regard to the effects of BMPs on osteoclasts, BMP-4 overexpression in bone[12] and deletion of the gene encoding a BMP antagonist, twisted gastrulation,[13] increase osteoclast number and thereby decrease bone volume. Overexpression of noggin in bone, another BMP antagonist, decreases osteoclast number and thereby increases bone volume.[12] These findings suggest that BMPs in bone enhance osteoclast formation and decrease bone volume. BMPs enhance osteoclast formation both directly and indirectly through osteoblasts. In vitro studies show that BMPs directly enhance osteoclast formation, and osteoclasts express BMP receptors.[14–19] Tamoxifen-dependent osteoblast-specific ablation of the *Bmpr1a* gene mediated by the type 1 collagen gene (*Col1a1*) promoter-CreER decreases osteoclast number and bone-resorption activity in mice.[20,21] Loss of BMPR1A signaling in osteoblasts reduced RANKL expression and increased osteoprotegerin (OPG) expression in osteoblasts, leading to impaired osteoclast formation.

Not only do osteoclasts resorb bone, but they are also considered to regulate osteoblast differentiation in the bone-remodeling process in vivo. To investigate the direct effects of BMPs on osteoclasts in vivo, we used floxed *Bmpr1a* mice[22] and a Cre knock-in mouse line to the *cathepsin K* locus ($Ctsk^{Cre/+}$)[23] to generate $Ctsk^{Cre/+}$;$Bmpr1a^{flox/flox}$ conditional knockout mice in which *Bmpr1a* is deleted in differentiated osteoclasts ($Bmpr1a^{\Delta Oc/\Delta Oc}$). The *Bmpr1a* gene was deleted after formation of osteoclasts in $Bmpr1a^{\Delta Oc/\Delta Oc}$ mice. Bone histomorphometric analysis revealed increased bone volume associated with markedly increased osteoblastic bone-formation rate (BFR) in the secondary spongiosa of $Bmpr1a^{\Delta Oc/\Delta Oc}$ mice. These results suggest that the loss of BMP signals within osteoclasts increases osteoblastic bone-formation activity.

## Materials and Methods

### Generation of conditional knockout mice

In order to generate *Bmpr1a* conditional knockout mice, *Ctsk-Cre* knock-in mice ($Ctsk^{Cre/+}$)[23] and $Bmpr1a^{flox/flox}$ mice[22] were prepared. The *Col1a1-Cre* transgene construct was created by replacing the *Bmp4* cDNA sequence of the *Col1a1-Bmp4* transgene constructs bearing the 2.3-kb *Col1a1* promoter sequence[12] with the Cre sequence. *Col1a1-Cre* transgenic mice were generated by microinjection of the *Col1a1-Cre* transgene into fertilized ova. $Bmpr1a^{flox/flox}$ mice were mated with $Ctsk^{Cre/+}$ or *Col1a1-Cre* mice to generate $Ctsk^{Cre/+}$;$Bmpr1a^{flox/+}$ or *Col1a1-Cre*;$Bmpr1a^{flox/+}$ mice, respectively. $Ctsk^{Cre/+}$;$Bmpr1a^{flox/+}$ mice were mated with $Ctsk^{Cre/+}$ to generate $Ctsk^{Cre/Cre}$;$Bmpr1a^{flox/+}$ mice. Then $Ctsk^{Cre/Cre}$;$Bmpr1a^{flox/+}$ and $Bmpr1a^{flox/+}$ mice were intercrossed and *Col1a1-Cre*;$Bmpr1a^{flox/+}$ and $Bmpr1a^{flox/flox}$ mice were intercrossed to generate $Ctsk^{Cre/+}$;$Bmpr1a^{flox/flox}$ mice and *Col1a1-Cre*;$Bmpr1a^{flox/flox}$ mice, respectively. $Ctsk^{Cre/+}$;$Bmpr1a^{+/+}$ mice and $Bmpr1a^{flox/flox}$ mice were used as controls. For genotyping, genomic DNA was isolated from tail tips and was subjected to PCR analysis according to the methods described previously for the *Cre* transgene[23,24] and *Bmpr1a* allele.[22]

All our animal experiments were approved by the Institutional Review Board of Osaka University Graduate School of Medicine.

### Micro–computed tomographic (μCT) analysis

Tibias were dissected and scanned using a microfocus X-ray CT system (SMX-100CT-SV, Shimadzu, Kyoto, Japan). The proximal metaphyseal region and the diaphyseal region were scanned at the following resolutions: 18.7 μm for 2-week-old tibias, 22.9 μm for 3.5-week-old tibias, 25.5 μm for 8-week-old tibias, and 25.7 μm for 12-week-old tibias. Data were reconstructed to produce images of the tibia using 3D visualization and measurement software (Vay Tek, Inc., Fairfield, IA, USA).

### Osteoclast culture

Induction of osteoclasts from bone marrow–derived cells was performed as described previously[25] with some modification. Bone marrow flushed from femurs and tibias was isolated and dissociated from mice aged 8 weeks. The resulting cells were seeded on 10-cm dishes, and nonadhering cells were collected the next day. Collected cells then were cultured for 3 days in the presence of 30 ng/mL of macrophage colony–stimulating factor (M-CSF; Pepro-Tech, Rocky Hill, NJ, USA). Adherent cell populations containing macrophages were subjected to extraction of genomic DNA (day 0) or were further cultured for 1, 4, and 8 days with 30 ng/mL of M-CSF and 4 nM RANKL (Oriental Yeast, Tokyo, Japan) followed by genomic DNA extraction. Genomic DNAs were extracted using a DNeasy Blood amd Tissue Kit (Qiagen, Valencia, CA, USA). Genomic DNAs were subjected to PCR amplification with a primer pair specific for the *Bmpr1a* gene. As an internal control, a 590-bp region of the endogenous

mouse *Rapsyn* gene[26] also was amplified from the genomic DNAs.

Induction of osteoclasts from spleen-derived cells was performed as described previously[27] with some modification. Spleen cells were isolated and dissociated from mice aged 6 weeks. The resulting cells were cultured in the presence of 30 ng/mL of M-CSF and 1 to 4 nM RANKL for the indicated number of days and were subjected to tartrate-resistant acid phosphatase (TRACP) staining.

In order to test resorption activity, osteoclasts were formed in the presence of 30 ng/mL of M-CSF and 4 nM RANKL on 16-well hydroxyapatite-coated slides (Osteologic, Becton Dickinson, Franklin Lakes, NJ, USA) for 18 days, and the resorption area was calculated by computer-assisted image analysis. Survival of osteoclasts was measured as reported previously.[28] After osteoclasts were formed using 30 ng/mL of M-CSF and 4 nM RANKL, cells were incubated in the absence of M-CSF and RANKL for the indicated times and were stained with TRACP. Numbers of morphologically intact $TRACP^+$ multinucleated cells were counted. The mean number of osteoclasts at formation was set at 1.

After formation of multinucleated osteoclasts, cells were replated to increase osteoclast purity, followed by extraction of total RNAs.

Coculture experiments were performed using previously described methods.[29,30] Briefly, primary osteoblasts ($10^4$ cells/$cm^2$) prepared from neonatal calvaria were cocultured with spleen cells ($5 \times 10^5$ cells/$cm^2$) from mice at 6 weeks of age in $\alpha$-MEM containing 10% fetal calf serum (FCS) and $10^{-8}$ M 1$\alpha$,25-dihydroxyvitamin $D_3$ [1,25$(OH)_2D_3$] in 48-well plates.

Osteoclast differentiation was evaluated by TRACP staining. Multinucleated $TRAcP^+$ cells with three or more nuclei were counted under a microscope. For examination of actin ring formation, cells were cultured on culture slides and fixed in 4% paraformaldehyde for 20 minutes. After fixation, cells were washed with 0.2% Triton X-100 PBS and incubated with 0.2 U/mL of rhodamine pharoidin (Molecular Probes, Invitrogen, Carlsbad, CA, USA) for 30 minutes and washed in PBS.

### Histologic analysis

Mice were dissected and tissue samples were fixed in 4% paraformaldehyde and dehydrated. Samples were decalcified, processed, embedded in paraffin, and sectioned. Semithin serial sections were stained with hematoxylin and eosin (H&E) and were subjected to TRACP staining using a TRAP staining kit (Primary Cell, Hokkaido, Japan). Immunohistochemistry was performed as described previously[31] using anti-Cre antibody (PRB-106C, dilution 1:500; Covance, Princeton, NJ, USA), anti-Osterix antibody (Ab22552, dilution 1:100; Abcam, Cambridge, UK), and anti-BMPR1A antibody (PAB-10536, dilution 1:50, Orbigen, San Diego, CA, USA). Immune complexes were detected with DAB+ (diaminobenzidine; K3467, Dako, Denmark) as a chromogen. For immunohistochemical analysis of sclerostin, antisclerostin antibody (AF1589, dilution 1:20; R&D Systems, Minneapolis, MN, USA) was used. Immune complexes were detected with Alexa Fluor 546 anti-goat (Invitrogen, Carlsbad, CA, USA).

### Histomorphometric analysis

Dynamic histomorphometric indices were determined by double fluorescence labeling in tibias. Eight-week-old mice were administered tetracycline intraperitoneally (20 mg/kg of body weight; Sigma-Aldrich, St Louis, MO, USA), followed 72 hours later by administration of a calcein label (10 mg/kg of body weight; Wako, Osaka, Japan). Mice were euthanized 36 hours after calcein administration. Hind limb bones were fixed with ethanol, embedded in methyl methacrylate, and sectioned. Sections were examined using a fluorescence microscope. Histomorphometric analyses were performed by staff at the Ito Bone Histomorphometry Institute (Niigata, Japan).

Four-week-old mice also were euthanized, and their vertebrae were processed similarly in order to analyze osteoclast numbers and erosive surface.

### Staining for β-galactosidase activity

β-Galactosidase activity was analyzed by staining with X-gal (5-bromo-4-chloro-3-indolyl-b-D-galactopyranoside; Sigma, St Louis, MO, USA), as described previously.[32]

### Real-time RT-PCR analysis

Total RNA was extracted from cultured osteoclasts and primary osteoblasts using an RNeasy Mini Kit (Qiagen, Santa Clarita, CA, USA). RNA was digested with DNase in order to eliminate contaminating genomic DNA before real-time quantitative RT-PCR. RNA samples were further purified using RNeasy Mini Kits (Qiagen). One microgram of total RNA was reverse transcribed into first-strand cDNA using SuperScript III (Invitrogen) and random hexamers. PCR amplification was carried out in a reaction volume of 20 μL containing 2 μL of cDNA, 10 μL of SYBER PremixExTaq (Takara, Shiga, Japan) and 7900HT (Applied BioSystems, Inc., Foster City, CA, USA). For quantification of *Bmpr1a* expression, Taqman primers and probes for *Bmpr1a* (Mm00477650; TaqMan Gene Expression Assays, Applied Biosystems, Carlsbad, CA, USA) and *Gapdh* (4352339E; Pre-Developed TaqMan Assay Regent Mouse *Gapd*) were used. RNA expression levels were normalized against levels of *Gapdh* expression. Mean relative expression levels in samples prepared from $Bmpr1a^{+/+}$ mice were set at 1. Primer pairs are listed in Supplemental Table S1.

### Statistical analysis

Results are expressed as means ± SD. Unpaired *t* test was used to compare data, and a *p* value of less than 0.05 was considered to indicate significance.

## Results

### Trabecular bone was thickened in $Bmpr1a^{\Delta Oc/\Delta Oc}$ mice

In order to delete *Bmpr1a* in an osteoclast-specific manner, we bred a floxed *Bmpr1a* mouse line[20] with a knock-in mouse line for Cre to the *Ctsk* locus.[21] Homozygous mice for the knock-in allele ($Ctsk^{Cre/Cre}$) are also homozygous null mice for *Ctsk* and show an osteopetrosis phenotypes owing to impaired

osteoclastic bone resorption.[23,33] The heterozygous mice for *Ctsk* show no overt phenotypes in bones,[21] but we bred $Ctsk^{Cre/Cre}$;$Bmpr1a^{flox/+}$ and $Bmpr1a^{flox/+}$ mice in order to exclude possible effects of different expression levels of *Ctsk* between $Ctsk^{Cre/+}$ and $Ctsk^{+/+}$ on phenotypes. We thus were able to directly compare the impact of the loss of BMPR1A signaling in osteoclasts in the $Ctsk^{Cre/+}$ background. Numbers of pups derived from $Ctsk^{Cre/Cre}$;$Bmpr1a^{flox/+}$ and $Bmpr1a^{flox/+}$ intercrosses were 74 $Ctsk^{Cre/+}$;$Bmpr1a^{+/+}$ mice ($Bmpr1a^{+/+}$), 133 $Ctsk^{Cre/+}$;$Bmpr1a^{flox/+}$ mice ($Bmpr1a^{\Delta Oc/+}$), and 69 $Ctsk^{Cre/+}$;$Bmpr1a^{flox/flox}$ mice ($Bmpr1a^{\Delta Oc/\Delta Oc}$). Thus $Bmpr1a^{\Delta Oc/\Delta Oc}$ mice were born with the expected Mendelian frequency. $Bmpr1a^{\Delta Oc/\Delta Oc}$ mice exhibited dwarfism when compared with $Bmpr1a^{+/+}$ mice (Fig. 1*A*) and $Bmpr1a^{\Delta Oc/+}$ mice, but there were no overt differences in appearance between $Bmpr1a^{+/+}$ mice and $Bmpr1a^{\Delta Oc/+}$ mice. The weight of $Bmpr1a^{\Delta Oc/\Delta Oc}$ mice was lower than that of $Bmpr1a^{+/+}$ mice (Fig. 1*B*). μCT analysis showed that trabecular bone thickness of the tibias of $Bmpr1a^{\Delta Oc/\Delta Oc}$ mice did not clearly differ from that of $Bmpr1a^{+/+}$ mice at 2 weeks of age (Fig. 1*C*). However, $Bmpr1a^{\Delta Oc/\Delta Oc}$ mice showed

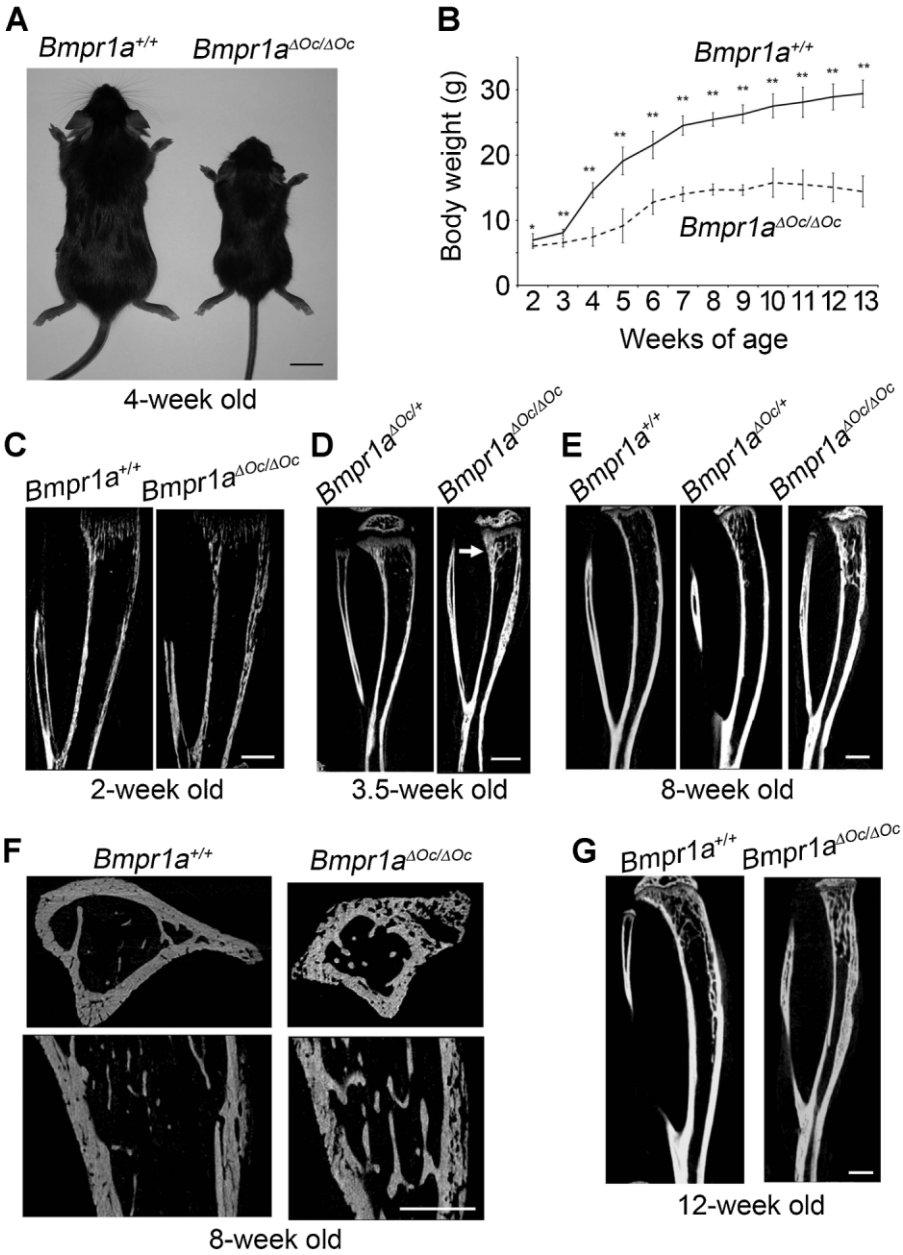


**Fig. 1.** Generation of $Bmpr1a^{\Delta Oc/\Delta Oc}$ conditional knockout mice and their bone phenotypes. $Ctsk^{Cre/Cre}$;$Bmpr1a^{flox/+}$ and $Bmpr1a^{flox/+}$ were intercrossed to generate $Ctsk^{Cre/+}$;$Bmpr1a^{+/+}$ mice ($Bmpr1a^{+/+}$), $Ctsk^{Cre/+}$;$Bmpr1a^{flox/+}$ mice ($Bmpr1a^{\Delta Oc/+}$), and $Ctsk^{Cre/+}$;$Bmpr1a^{flox/flox}$ mice ($Bmpr1a^{\Delta Oc/\Delta Oc}$). (*A*) Photograph of $Bmpr1a^{+/+}$ mice and $Bmpr1a^{\Delta Oc/\Delta Oc}$ mice at 4 weeks of age. (*B*) Growth curves of $Bmpr1a^{+/+}$ mice and $Bmpr1a^{\Delta Oc/\Delta Oc}$ mice ($n = 8$ each). $^{*}p < 0.05$; $^{**}p < 0.01$ between $Bmpr1a^{+/+}$ mice and $Bmpr1a^{\Delta Oc/\Delta Oc}$ mice. (*C–G*) μCT analysis of tibia at 2 weeks (*C*), 3.5 weeks (*D*), 8 weeks (*E*, *F*), and 12 weeks (*G*) of age. Reconstructed sagittal view of tibia (*C–E*, *G*). Reconstructed axial (*F*, *top panels*) and sagittal (*F*, *bottom panels*) views of proximal metaphyseal regions of tibia. (*D*) $Bmpr1a^{\Delta Oc/\Delta Oc}$ mice started to show thick trabecular bone in the proximal region at 3.5 weeks of age (*arrow*). Scale bars = (*A*) 1 cm, (*C–G*) 1 mm.

thick trabecular bone in the proximal region when compared with *Bmpr1a*$^{\Delta Oc/+}$ mice at 3.5 weeks of age, as evidenced by μCT images (Fig. 1*D*, *arrow*). Trabecular bone of the proximal tibia was thicker in *Bmpr1a*$^{\Delta Oc/\Delta Oc}$ mice compared with *Bmpr1a*$^{+/+}$ mice and *Bmpr1a*$^{\Delta Oc/+}$ mice at 8 weeks of age (Fig. 1*E*). Bone marrow spaces were narrower and cortical bone was more porotic in *Bmpr1a*$^{\Delta Oc/\Delta Oc}$ mice compared with *Bmpr1a*$^{+/+}$ mice at 8 weeks of age (Fig. 1*F*). Trabecular bone in the proximal tibia also was thick in *Bmpr1a*$^{\Delta Oc/\Delta Oc}$ mice compared with *Bmpr1a*$^{+/+}$ mice at 12 weeks of age (Fig. 1*G*).

## *Bmpr1a* gene was specifically deleted in differentiated osteoclasts in *Bmpr1a*$^{\Delta Oc/\Delta Oc}$ mice

In order to analyze Cre expression patterns in *Bmpr1a*$^{\Delta Oc/\Delta Oc}$ bone, we performed immunohistochemical analysis. Immunoreactivity for Cre was not detected in samples from negative-control *Bmpr1a*$^{flox/flox}$ mice (Supplemental Fig. S1*A*, *left panel*) but was specifically detected in multinucleated cells in *Bmpr1a*$^{\Delta Oc/\Delta Oc}$ mouse tibial bone at 2 days of age (Supplemental Fig. S1*A*, *right panel*, and *B*, *left panels*, *arrowheads*). TRACP staining in the adjacent section showed that Cre-expressing cells were TRACP$^{+}$ multinucleated cells (Supplemental Fig. S1*B*, *upper panels*, *arrowheads*). Of 85 Cre-expressing cells in one section, 70 cells were recognized in the adjacent sections, and all 70 cells were TRACP$^{+}$. Immunohistochemical staining of other adjacent sections with antiosterix antibodies showed that Cre-expressing cells did not produce osterix (Supplemental Fig. S1*B*, *lower panels*, *arrowheads*). Osteoblasts on the surface of bone matrix expressed osterix (Supplemental Fig. S1*B*, *lower right panel*, *asterisks*) and were not stained with antibody against Cre recombinase (Supplemental Fig. S1*B*, *lower left panel*). Immunoreactivity for Cre also was specifically detected in multinucleated cells in *Bmpr1a*$^{\Delta Oc/\Delta Oc}$ mouse tibial bone at 8 weeks of age (Supplemental Fig. S1*C*, *top panel*). Adjacent sections showed that Cre-expressing cells were TRACP$^{+}$ and osterix$^{-}$ (Supplemental Fig. S1*C*, 1st, *first and third panels*, *arrowheads*). These results indicate that Cre is specifically expressed in multinucleated osteoclasts but not in osteoblasts.

Immunoreactivity for BMPR1A was detected in osteoclasts (Supplemental Fig. S1*D*, *left top*, *half-arrow*), which were identified by TRACP staining in serial sections (Supplemental Fig. S1*D*, *left bottom*, *half-arrow*) and osteoblasts in *Bmpr1a*$^{+/+}$ bone. On the other hand, immunoreactivity for BMPR1A antibodies was lost only in osteoclasts (Supplemental Fig. S1*D*, *right top*, *arrow*), which were identified by TRACP staining in adjacent sections (Supplemental Fig. S1*D*, *right bottom*, *arrow*) in *Bmpr1a*$^{\Delta Oc/\Delta Oc}$ bone. These results further confirmed that *Bmpr1a*$^{\Delta Oc/\Delta Oc}$ mice lost BMPR1A specifically in multinucleated osteoclasts.

In order to confirm that *Bmpr1a* was deleted in differentiated osteoclasts but not in osteoclast precursor cells, we examined deletion of the *Bmpr1a* gene during the differentiation process of osteoclasts in vitro. We harvested bone marrow cells from mice and cultured them in the presence of M-CSF. The resulting adhering cells containing macrophages were further cultured in the presence of M-CSF and RANKL to induce osteoclasts, followed by genomic DNA extraction. Multinucleated osteoclasts were formed around 4 to 5 days after the addition of RANKL. Genomic DNAs were subjected to PCR amplification using a pair of primers, fx1 and fx4,[22] designed for the upstream and downstream regions of the two *loxP* sites flanking exon 2 (Supplemental Fig. S2*A*). Genomic DNA extracted from *Bmpr1a*$^{+/+}$ bone marrow cells produced a 2.2-kb band but no 180-bp products before (day 0) or at 1, 4, and 8 days after addition of RANKL (Supplemental Fig. S2*B*). Genomic DNA from *Bmpr1a*$^{\Delta Oc/\Delta Oc}$ bone marrow cells produced the 2.2-kb band and no 180-bp band before addition of RANKL (day 0). The absence of the 180-bp band indicates no recombination in these cells. On the other hand, 1 day after addition of RANKL, a trace of the 180-bp band was detected (Fig. 3*B*). Four days after addition of RANKL, the 2.2-kb band decreased in intensity, whereas the 180-bp band increased in intensity. Furthermore, 8 days after the addition of RANKL, the 2.2-kb products almost completely disappeared, and the intensity of the 180-bp band increased. The 180-bp band corresponds to the genomic fragment from which the *Bmpr1a* exon 2 sequence is excised after recombination at *loxP* sites. These results suggest that *Bmpr1a*$^{\Delta Oc/\Delta Oc}$ cells lacked *Bmpr1a* in differentiated osteoclasts but not in osteoclast precursors.

## Osteoblastic bone formation was markedly increased in remodeling trabecular bone from *Bmpr1a*$^{\Delta Oc/\Delta Oc}$ mice

We prepared histologic sections of the proximal tibia and performed TRACP staining. The number of osteoclasts indicated by TRACP staining was higher in proximal tibias in *Bmpr1a*$^{\Delta Oc/\Delta Oc}$ mice than in *Bmpr1a*$^{+/+}$ mice at 3 weeks of age (Fig. 2*A*). Histomorphometric analysis showed increased osteoclast number and increased erosive surface in trabecular bone in the third lumber vertebral bodies of 4-week-old mice (Fig. 2*B*). Narrow bone marrow spaces were associated with reductions in osteoclast numbers on the endosteum of *Bmpr1a*$^{\Delta Oc/\Delta Oc}$ mice (Fig. 2*C*, *arrows*). Increased cavities within the cortical bone of *Bmpr1a*$^{\Delta Oc/\Delta Oc}$ mice contained osteoclasts (Fig. 2*C*, *arrowheads*). Since cortical porosity with increased osteoclast number in the cavities is recognized in mice treated with parathyroid hormone (PTH),[34,35] it is possible that PTH signals are upregulated in *Bmpr1a*$^{\Delta Oc/\Delta Oc}$ bone. We analyzed the expression of sclerostin, whose expression is known to be reduced by PTH.[36] There were no substantial differences in sclerostin expression in osteocytes between *Bmpr1a*$^{\Delta Oc/\Delta Oc}$ mice and *Bmpr1a*$^{+/+}$ mice on immunohistochemical analysis (Fig. 2*D*), thus suggesting that PTH signals appeared normal in *Bmpr1a*$^{\Delta Oc/\Delta Oc}$ mice.

Osteoclast numbers were lower in trabecular bone in proximal tibias in *Bmpr1a*$^{\Delta Oc/\Delta Oc}$ mice compared with *Bmpr1a*$^{+/+}$ mice at 8 weeks of age (Fig. 3*A*). We next performed histomorphometric analysis of the remodeling trabecular bone at 8 weeks of age in order to quantitatively examine bone turnover. Bone volume increased markedly and was associated with significantly higher osteoblast number and BFR along with decreased osteoclast number and erosive surface in *Bmpr1a*$^{\Delta Oc/\Delta Oc}$ mice compared with *Bmpr1a*$^{+/+}$ mice (Fig. 3*B–D*). Osteoid volume also was higher. Histology of *Bmpr1a*$^{\Delta Oc/\Delta Oc}$ trabeculae showed that trabecular bone was markedly thick, particularly in area of secondary spongiosa, compared with the areas of primary

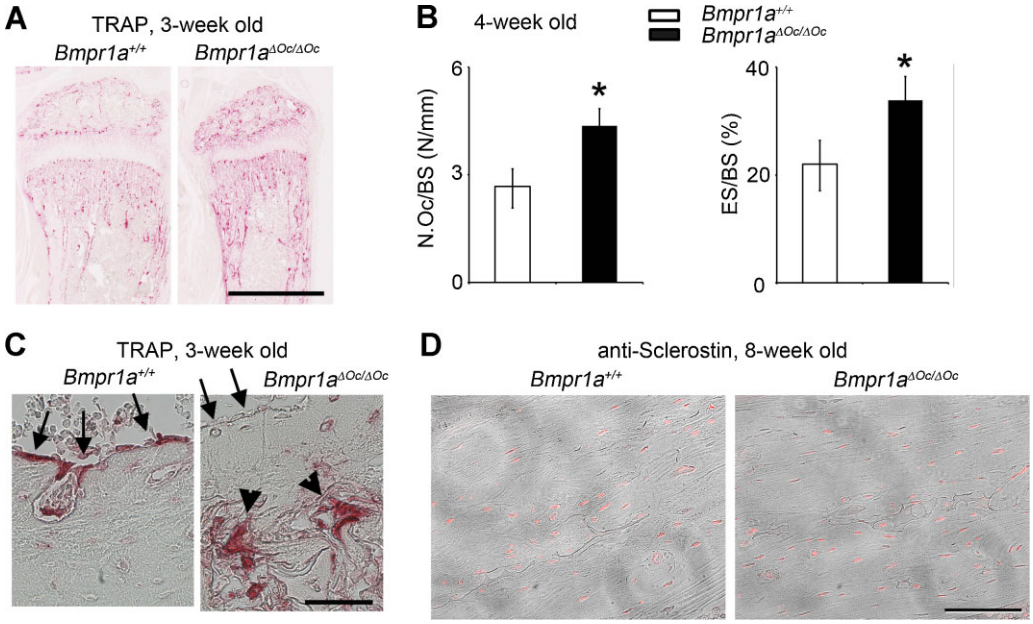


**Fig. 2.** Histomorphometric analysis of bone from *Bmpr1a*$^{+/+}$ mice and *Bmpr1a*$^{\Delta Oc/\Delta Oc}$ mice. (*A*) Sagittal sections of proximal tibia at 3 weeks of age were subjected to TRACP staining. Scale bar, 1 mm. (*B*) Bone histomorphometry of the third lumbar vertebral bodies at 4 weeks of age ($n = 3$ each). $^{*}p < 0.05$ between *Bmpr1a*$^{+/+}$ mice and *Bmpr1a*$^{\Delta Oc/\Delta Oc}$ mice. Osteoclast number per bone surface area (N.Oc/B) and eroded surface area per bone surface area (ES/BS). (*C*) Axial sections of middle of tibia at 3 weeks of age were subjected to TRACP staining. Scale bar, 50 μm. (*D*) Histologic sections of tibia of *Bmpr1a*$^{flox/flox}$ and *Bmpr1a*$^{\Delta Oc/\Delta Oc}$ mice at 8 weeks of age were immunostained using antisclerostin antibodies (*orange*). Scale bar = 100 μm.

spongiosa at 8 weeks of age (Fig. 3*D*, *right panel*). Immunohistochemical analysis confirmed increased numbers of osteoblasts, which were identified by immunostaining with the antiosterix antibody at 8 weeks of age (Fig. 3*E*). In summary, at 8 weeks of age when bone remodeling occurs, deletion of *Bmpr1a* in differentiated osteoclasts increases osteoblastic bone formation and decreases osteoclastic bone resorption, thereby substantially increasing bone volume in trabecular bone.

## *Bmpr1a* deletion in osteoblasts reduces osteoblastic bone formation

In order to determine whether osteoclasts lacking BMPR1A signaling enhance osteoblastic bone formation during bone remodeling, we needed to ensure that the osteoblast phenotype found in the *Bmpr1a*$^{\Delta Oc/\Delta Oc}$ mice was not caused by deletion of *Bmpr1a* in osteoblasts in the mice. For this purpose, we first generated *Col1a1-Cre* transgenic mice bearing the osteoblast-specific 2.3-kb *Col1a1* promoter sequence.[37] By mating with *CAG promoter-flox-CAT-flox-LacZ* transgenic tester mice,[38] our *Col1a1-Cre* transgenic mice were shown to direct Cre-mediated recombination specifically to bone at 17.5 days after coitum (Fig. 4*A*, *left panels*). Histologic analysis confirmed the specific recombination in osteoblasts (Fig. 4*A*, *right panel*).

By crossing *Col1a1-Cre* transgenic mice with floxed *Bmpr1a* mice, we generated *Col1a1-Cre;Bmpr1a*$^{flox/flox}$ conditional knockout mice (*Bmpr1a*$^{\Delta Ob/\Delta Ob}$). *Bmpr1a*$^{\Delta Ob/\Delta Ob}$ mice developed dwarfism after birth. μCT analysis showed that trabecular bone was thick in *Bmpr1a*$^{\Delta Ob/\Delta Ob}$ mouse tibias compared with control *Bmpr1a*$^{flox/flox}$ mice at 5 weeks of age (Fig. 4*B*). Histologic analysis revealed that bone volume had already increased at 2 days after birth (Fig. 4*C*). Immunoreactivity against anti-Cre antibody was not detected in osteoclasts, which were identified by TRACP staining (Fig. 4*D*, *E*), and was detected in osteoblasts, indicated by osterix expression (Fig. 4*D*, *F*), in *Bmpr1a*$^{\Delta Ob/\Delta Ob}$ mice. Histology of *Bmpr1a*$^{\Delta Ob/\Delta Ob}$ trabeculae showed that trabecular bone was markedly thick in both primary and secondary spongiosa areas (Fig. 4*G*). Immunohistochemical staining using antiosterix antibodies confirmed increased numbers of osteoblasts in *Bmpr1a*$^{\Delta Ob/\Delta Ob}$ bone (Fig. 4*H*). TRACP staining revealed markedly decreased numbers of osteoclasts in *Bmpr1a*$^{\Delta Ob/\Delta Ob}$ bone (Fig. 4*H*).

Bone histomorphometric analysis confirmed markedly increased bone volume associated with significantly increased osteoblast number and decreased osteoclast number and an erosive surface in *Bmpr1a*$^{\Delta Ob/\Delta Ob}$ mice compared with *Bmpr1a*$^{flox/flox}$ mice at 8 weeks of age (Fig. 4*I*). BFR was markedly decreased (almost zero under the conditions used in this study with a labeling interval of 3 days) in *Bmpr1a*$^{\Delta Ob/\Delta Ob}$ mice compared with *Bmpr1a*$^{flox/flox}$ mice. Thus *Bmpr1a*$^{\Delta Ob/\Delta Ob}$ mice showed osteopetrotic changes with low bone turnover. These changes are consistent with but more marked than in a previous report showing that osteoclast number decreases in tamoxifen-dependent *Col1a1-CreER;Bmpr1a*$^{flox/flox}$ bone.[20] There were no significant differences in these bone parameters between respective control mice (*Bmpr1a*$^{+/+}$ mice and *Bmpr1a*$^{flox/flox}$ mice; comparison between Figs. 3*B* and 4*I*). *Bmpr1a*$^{\Delta Ob/\Delta Ob}$ osteoblasts expressed osterix (Fig. 4*H*, *right top*), thus suggesting that osteoblasts without intrinsic BMPR1A signaling differentiate to some extent but have markedly reduced bone-forming activities. The opposite changes in BFR between *Bmpr1a*$^{\Delta Ob/\Delta Ob}$ mice and *Bmpr1a*$^{\Delta Oc/\Delta Oc}$ mice strongly

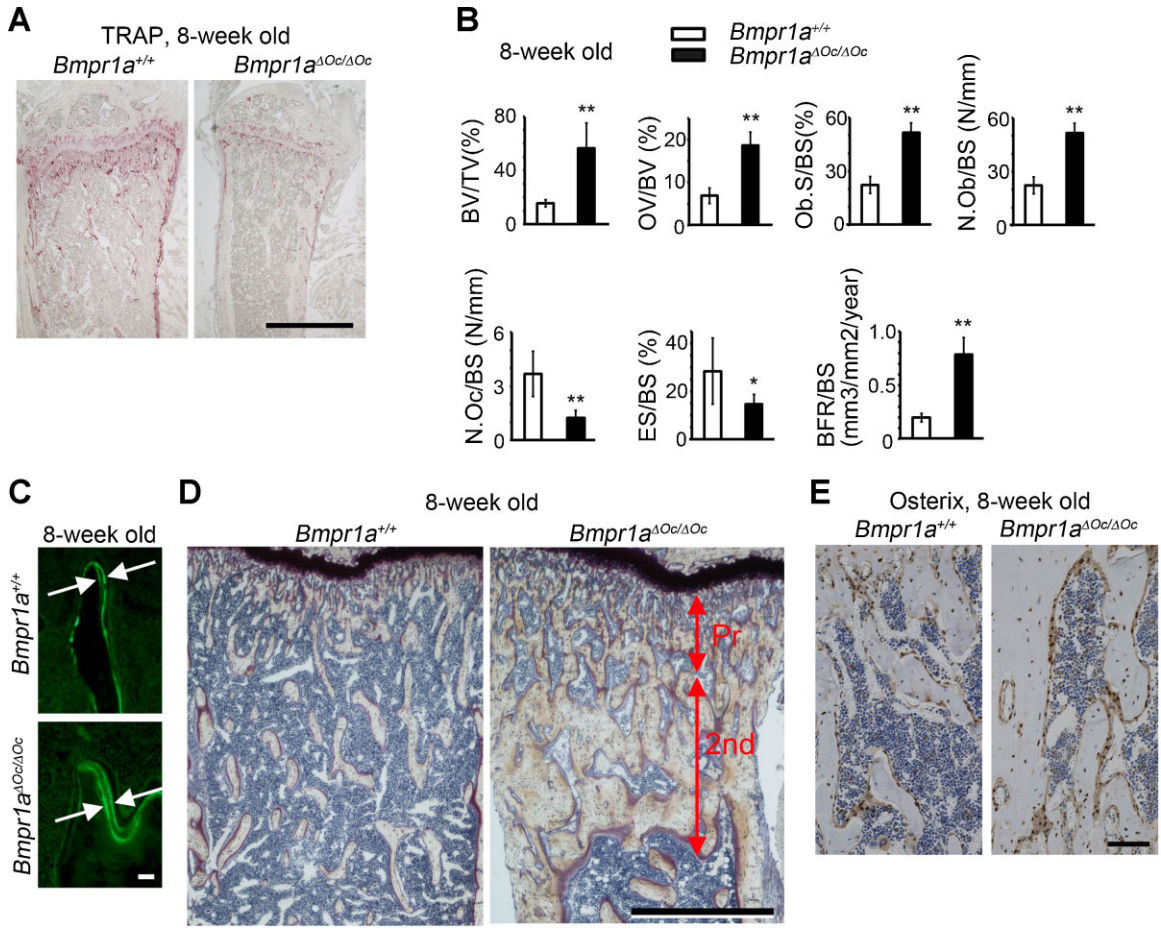


**Fig. 3.** (*A*) Sagittal sections of proximal tibia at 8 weeks of age were subjected to TRACP staining. Scale bar = 1 mm. (*B*) Bone histomorphometry of proximal tibia at 8 weeks of age ($n = 5$ for *Bmpr1a*$^{+/+}$ and $n = 6$ for *Bmpr1a*$^{\Delta Oc/\Delta Oc}$). $^{*}p < 0.05$; $^{**}p < 0.01$ between *Bmpr1a*$^{+/+}$ mice and *Bmpr1a*$^{\Delta Oc/\Delta Oc}$ mice. Trabecular bone volume per tissue volume (BV/TV), osteoid volume per bone volume (OV/BV), osteoblast surface area per bone surface area (Ob.S/BS), number of osteoblasts per bone surface area (N. Ob/BS), osteoclast number per bone surface area (N.Oc/B), eroded surface area per bone surface area (ES/BS), and bone formation rate per bone surface area (BFR/BS). (*C*) Fluorescence micrograph of labeled mineralization fronts in the proximal tibia at 8 weeks of age. *Arrows* indicate distance between two consecutive labels. Scale bar = 20 μm. (*D*) Villanueva bone staining of proximal tibia at 8 weeks of age. Note that trabecular bone was markedly thickened in the secondary spongiosa area (*2nd*) when compared with the primary spongiosa area (*Pr*) in *Bmpr1a*$^{\Delta Oc/\Delta Oc}$ mice. Scale bar = 1 mm. (*E*) Immunohistochemistry of proximal tibia at 8 weeks of age using antiosterix antibody. Scale bar = 20 μm.

support the conclusion that osteoclasts lacking BMPR1A signaling enhance osteoblastic bone formation during bone remodeling.

## Osteoclast formation was normal or slightly increased from *Bmpr1a*$^{\Delta Oc/\Delta Oc}$ spleen cells in vitro

In order to analyze the cell-autonomous effects of *Bmpr1a* deletion in differentiated osteoclasts, we induced osteoclasts in vitro from *Bmpr1a*$^{\Delta Oc/\Delta Oc}$ spleen cells in the presence of M-CSF and various concentrations of RANKL. There were no significant differences in osteoclast formation between *Bmpr1a*$^{\Delta Oc/\Delta Oc}$ and *Bmpr1a*$^{+/+}$ spleen cells in the presence of 4 or 3 nM RANKL (Fig. 5*A*). The mean number of osteoclasts formed from *Bmpr1a*$^{\Delta Oc/\Delta Oc}$ spleen cells was slightly but significantly higher than that from *Bmpr1a*$^{+/+}$ spleen cells in the presence of 2 or 1 nM RANKL. Increased osteoclast formation from *Bmpr1a*$^{\Delta Oc/\Delta Oc}$ spleen cells at low concentrations of RANKL suggests that deletion of *Bmpr1a* sensitizes osteoclast formation induced by RANKL. We did not find marked differences in actin ring formation (Fig. 5*B*) and hydroxyapatite resorption (Fig. 5*C*) between osteoclasts derived from *Bmpr1a*$^{\Delta Oc/\Delta Oc}$ and *Bmpr1a*$^{+/+}$ spleen cells owing to M-CSF and 4 nM RANKL. We did not observe marked differences in cell survival (Fig. 5*D*).

We then replated these osteoclasts formed in the presence of M-CSF and 4 nM RANKL to increase their purity (Fig. 6*A*) for expression analysis of the osteoclast marker genes (Fig. 6*B*). We extracted total RNA and subjected cells to real-time RT-PCR expression analysis. Expression levels of *Bmpr1a* were lower in osteoclasts induced from *Bmpr1a*$^{\Delta Oc/\Delta Oc}$ spleen cells than in those from *Bmpr1a*$^{+/+}$ spleen cells (Fig. 6*B*). Expression of *Tracp*, *Ctsk*, and *Mmp9* was higher in osteoclasts induced from *Bmpr1a*$^{\Delta Oc/\Delta Oc}$ spleen cells. Expression of *Nfatc1* was higher in osteoclasts induced from *Bmpr1a*$^{\Delta Oc/\Delta Oc}$ spleen cells. It is possible that *Bmpr1a* deletion increases *Nfatc1* expression, causing decreased expression of bone-resorption markers in osteoclasts. We then cocultured osteoblasts prepared from neonatal *Bmpr1a*$^{+/+}$ mouse calvaria with *Bmpr1a*$^{+/+}$ spleen cells

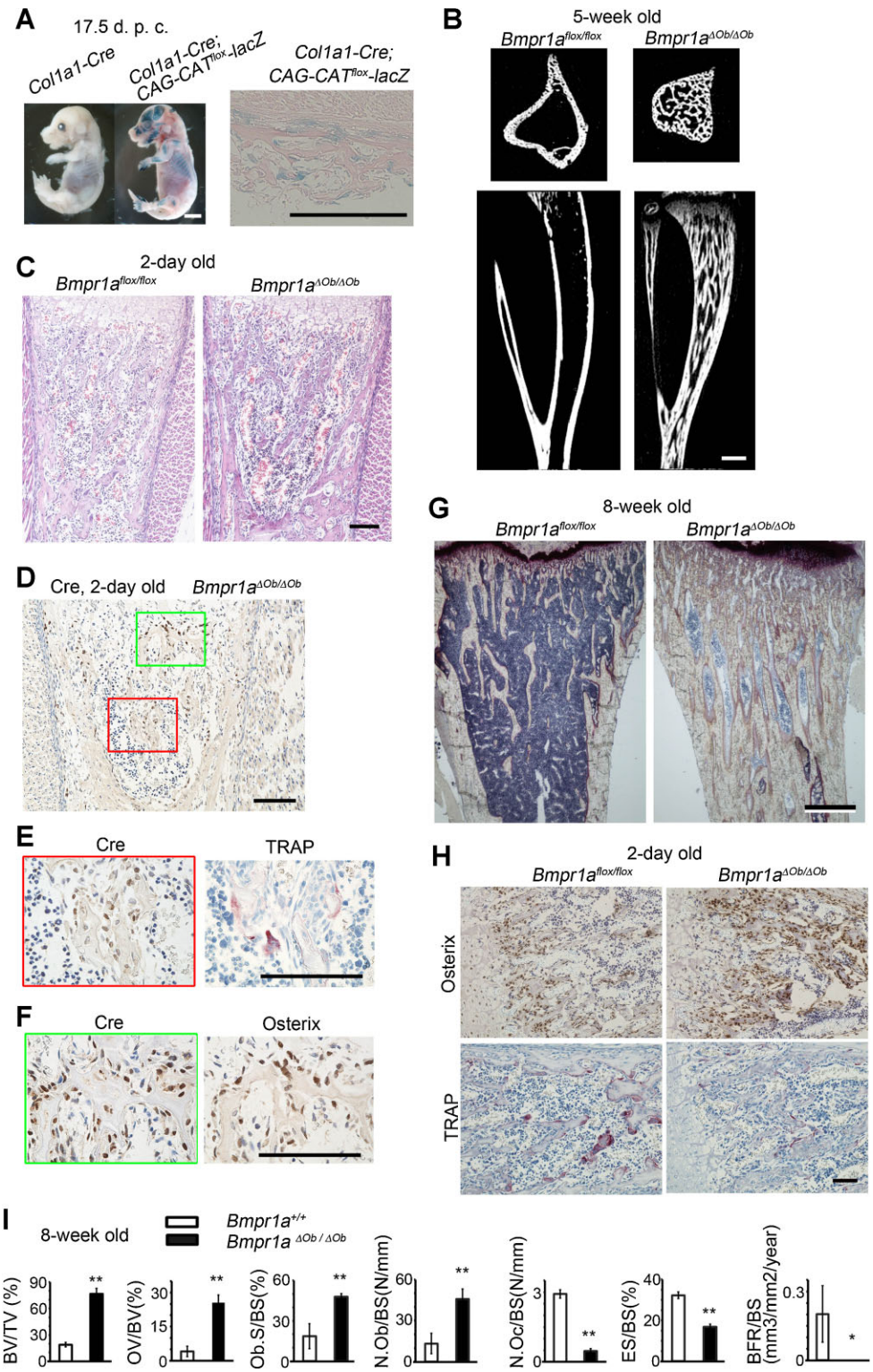


**Fig. 4.** Generation of *Bmpr1a*$^{\Delta Ob/\Delta Ob}$ mice. *Col1a1-Cre;Bmpr1a*$^{flox/+}$ and *Bmpr1a*$^{flox/flox}$ were intercrossed to generate *Bmpr1a*$^{flox/flox}$ mice, *Bmpr1a*$^{flox/+}$ mice, *Col1a1-Cre;Bmpr1a*$^{flox/+}$ mice, and *Col1a1-Cre;Bmpr1a*$^{flox/flox}$ mice (*Bmpr1a*$^{\Delta Ob/\Delta Ob}$). *Bmpr1a*$^{flox/flox}$ mice were used as controls. (*A*) Preparation of *Col1a1-Cre* transgenic mice. *Col1a1*-Cre transgenic mice were mated with *CAG-CAT*$^{floxed}$*-LacZ* tester mice, and the whole bodies of progeny at 17.5 days after coitum were examined for *LacZ* expression by X-gal staining (*left*). Histologic sections confirmed specific recombination in osteoblasts (*right*). Scale bars = (*left*) 2.5 mm; (*right*) 50 μm. (*B*) μCT analysis of tibia at 5 weeks of age.(*Above*) reconstructed axial view. (*Below*) Reconstructed sagittal view. Scale bar = 1 mm. (*C*) Histology of femur stained with hematoxylin and eosin at 2 days of age. Scale bar = 100 μm. (*D*) Immunohistochemical staining of tibia from *Bmpr1a*$^{\Delta Ob/\Delta Ob}$ mice at 2 days of age using anti-Cre antibodies. Scale bar = 100 μm. (*E*) (*Left*) Magnification of red boxed region in panel *E*. (*Right*) Serial sections were subjected to TRACP staining. Scale bar = 100 μm. ( *F*) (*Left*) Magnification of green boxed region in panel *E*. (*Right*) Serial sections were immunostained with antiosterix antibody. Scale bar = 100 μm. (*G*) Villanueva bone staining of proximal tibia at 8 weeks of age. Scale bar = 1 mm. (*H*) Histologic sections of proximal tibias at 2 days of age were immunostained with antiosterix antibody and subjected to TRACP staining. Scale bar = 50 μm. (*I*) Bone histomorphometric analysis of proximal tibias at 8 weeks of age ($n = 3$ each). $^{*}p < 0.05$; $^{**}p < 0.01$ between *Bmpr1a*$^{+/+}$ mice and *Bmpr1a*$^{\Delta Ob/\Delta Ob}$ mice.

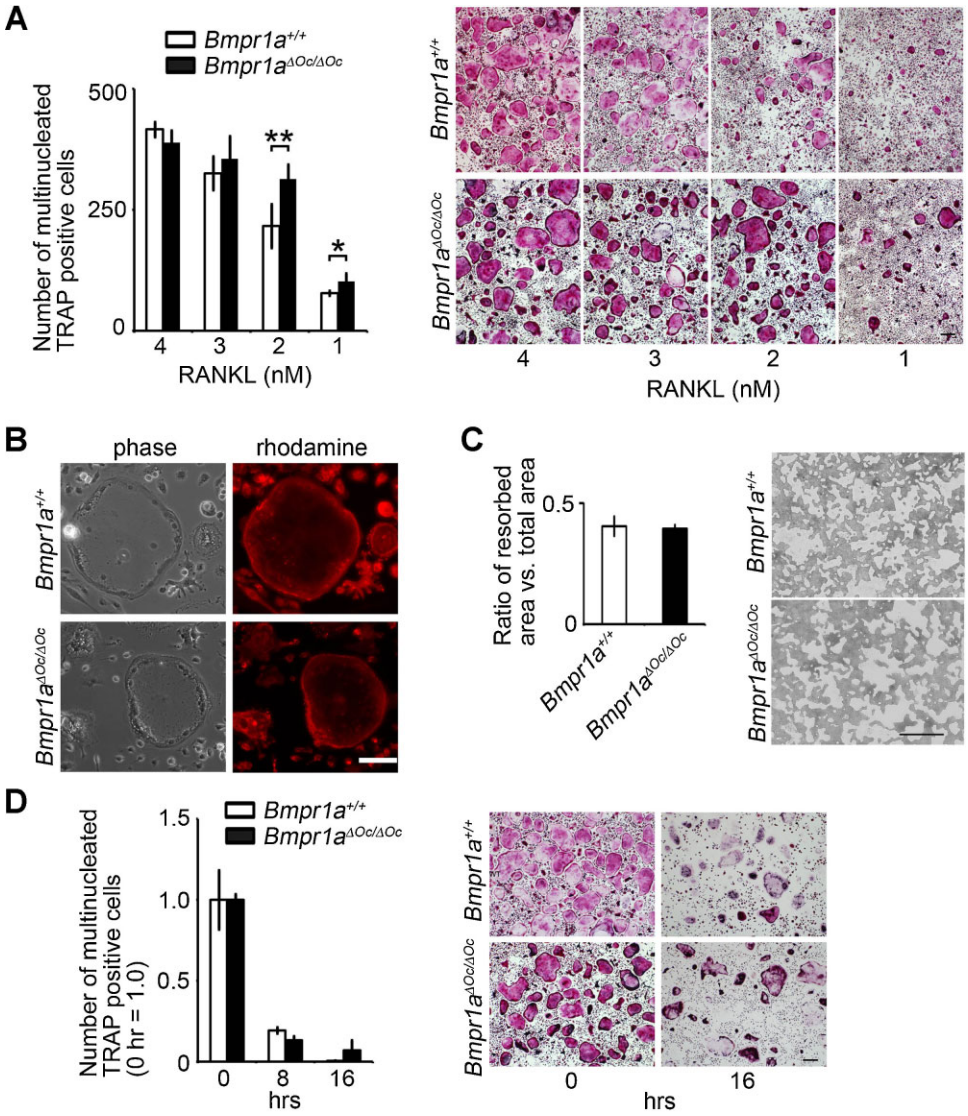


**Fig. 5.** In vitro osteoclast formation from *Bmpr1a*$^{\Delta Oc/\Delta Oc}$ spleen cells. (*A*) Spleen cells from *Bmpr1a*$^{+/+}$ mice and *Bmpr1a*$^{\Delta Oc/\Delta Oc}$ mice were cultured in the presence of M-CSF and various concentrations of RANKL for 5 days and were subjected to TRACP staining. (*Left*) Numbers of TRACP$^{+}$ cells with three or more nuclei ($n = 5$ each). $^{*}p < 0.05$; $^{**}p < 0.01$ between *Bmpr1a*$^{+/+}$ mice and *Bmpr1a*$^{\Delta Oc/\Delta Oc}$ mice. (*Right*) Images of culture. Scale bar = 200 μm. (*B*) Normal actin ring formation in osteoclasts induced from *Bmpr1a*$^{\Delta Oc/\Delta Oc}$ spleen cells by M-CSF and RANKL. Scale bar = 200 μm. (*C*) Resorption activities of *Bmpr1a*$^{\Delta Oc/\Delta Oc}$ osteoclasts on hydroxyapatite-coated slides (Osteologic, Becton Dickinson). (*Left*) Ratio of resorbed area versus total area ($n = 3$). $p = 0.35$ between *Bmpr1a*$^{+/+}$ mice and *Bmpr1a*$^{\Delta Oc/\Delta Oc}$ mice. (*Right*) Images of slides. Scale bar = 200 μm. (*D*) Survival of *Bmpr1a*$^{\Delta Oc/\Delta Oc}$ osteoclasts. After formation of osteoclasts owing to M-CSF and RANKL, cells were incubated in the absence of M-CSF and RANKL. (*Left*) TRACP$^{+}$ cells with three or more nuclei were counted ($n = 5$ for *Bmpr1a*$^{+/+}$ and $n = 4$ for *Bmpr1a*$^{\Delta Oc/\Delta Oc}$). Mean number of osteoclasts formed was set at 1. (*Right*) Images of culture. Scale bar = 200 μm.

or *Bmpr1a*$^{\Delta Oc/\Delta Oc}$ spleen cells. The number of osteoclasts was slightly but significantly higher in cocultures containing *Bmpr1a*$^{\Delta Oc/\Delta Oc}$ spleen cells than in cocultures containing *Bmpr1a*$^{+/+}$ spleen cells (Fig. 6*C*). These in vitro results collectively suggest that BMPR1A signals in differentiated osteoclasts suppress osteoclast differentiation.

## Discussion

In this report, we demonstrated that signaling through a type 1A BMP receptor, BMPR1A, in differentiated osteoclasts exhibits dual functions: (1) negatively regulating expression of bone-resorption markers, including *Mmp9* in differentiated osteoclasts induced by M-CSF and RANKL in vitro and (2) negatively regulating osteoblastic bone formation in vivo. Trabecular bone in the femur and tibia was consistently thickened in *Bmpr1a*$^{\Delta Oc/\Delta Oc}$ mice at 3.5, 8, and 12 weeks of age, and osteoblastic bone formation was higher in secondary spongiosa of *Bmpr1a*$^{\Delta Oc/\Delta Oc}$ mice at 8 weeks of age. We confirmed that expression of Cre is confined to differentiated osteoclasts but is not seen in immature osteoclasts or osteoblasts. Together with a previous study,[20] this study demonstrates that *Bmpr1a* deletion in osteoblasts markedly decreases osteoblastic bone formation. We thus may hypothesize that osteoclasts inhibit osteoblastic bone-formation activity in a BMPR1A signaling-dependent manner.

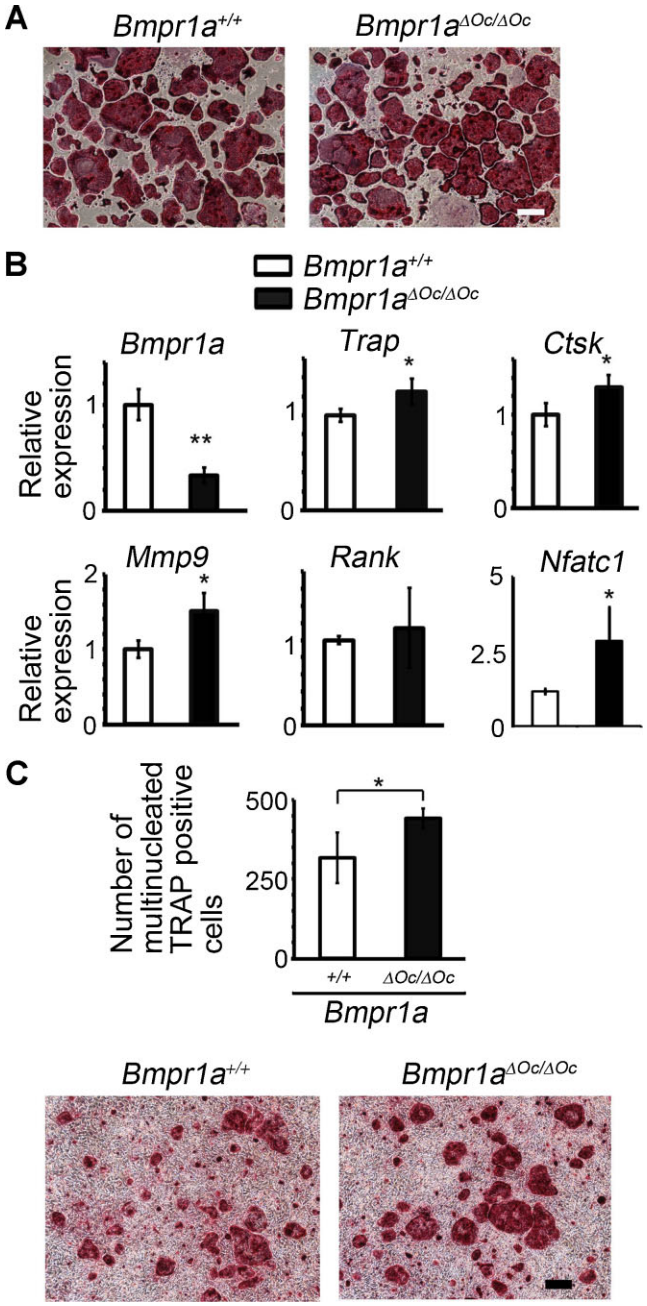


**Fig. 6.** Maker gene expression in *Bmpr1a*$^{\Delta Oc/\Delta Oc}$ osteoclasts and osteoclast formation in coculture with osteoblasts. (*A*) Osteoclasts induced from spleen cells by M-CSF and RANKL were replated. TRACP staining. Purity of osteoclasts increased after replating compared with before replating (*A*). Scale bar = 200 μm. (*B*) Marker gene expression analysis of replated osteoclasts by real-time RT-PCR ($n = 3$ each). (*C*) TRACP staining of osteoclasts in cocultures of primary osteoblasts prepared from *Bmpr1a*$^{+/+}$ mouse calvaria and cells prepared from *Bmpr1a*$^{+/+}$ or *Bmpr1a*$^{\Delta Oc/\Delta Oc}$ spleen. (*Left*) Numbers of TRACP$^{+}$ cells with three or more nuclei ($n = 4$ each). (*Right*) Images of culture. Scale bar = 200 μm. $^{*}p < 0.05$; $^{**}p < 0.01$ between *Bmpr1a*$^{+/+}$ mice and *Bmpr1a*$^{\Delta Oc/\Delta Oc}$ mice.

Previous in vitro studies suggested that the direct effect of BMPs on osteoclast lineage cells is to enhance osteoclast formation.[14–19] In this study, Cre was expressed in multinucleated osteoclasts in *Bmpr1a*$^{\Delta Oc/\Delta Oc}$ mice, and recombination generally started 4 days after addition of RANKL in vitro. These observations indicate that the *Bmpr1a* gene was deleted at later stages in the differentiation process of osteoclast-lineage cells, which may explain discrepancies in the effects of BMP signals on osteoclast formation between this study and previous studies. Our results revealed that deletion of BMPR1A signaling in differentiated osteoclasts increases expression of bone resorption markers, but not affects resorption acitivity on hydroxyapatite and survival of osteoclasts, which suggests that BMPR1A signaling slightly negatively regulates differentiation of osteoclasts. Taken ttogether with previous findings, our results suggest that BMPR1A signaling regulates osteoclasts differentially depending on the stage of the differentiation process for monocyte, macrophage, and osteoclast lineage cells. In trabecular bone of *Bmpr1a*$^{\Delta Oc/\Delta Oc}$ mice, osteoclast number increased at 3 to 4 weeks of age and decreased at 8 weeks of age. It is unclear why osteoclast number decreased at 8 weeks of age. We found that Cre is specifically expressed in multinucleated osteoclasts in the *Bmpr1a*$^{\Delta Oc/\Delta Oc}$ mice. However, it is still formally possible that *Bmpr1a* was deleted from cells other than osteoclasts, and formation of osteoclasts may have been affected by indirect effects of *Bmpr1a* loss in other types of cells.

The effects of BMPs on bone formation and metabolism have been studied extensively previously. However, examination of the in vivo effects of BMPs on each type of cell in bone revealed unexpected functions for BMPs. Deletion of BMPR1A signals in osteoblasts negatively influence osteoclast formation via regulation of canonical Wnt signaling, resulting in increased bone volume, as shown in both previous reports[20,21,39] and in this study. Our results also showed, for the first time, that deletion of BMPR1A signals in differentiated osteoclasts enhances osteoblastic bone formation, resulting in increased bone volume in mature trabecular bone area where bone remodeling occurs. *Bmpr1a*$^{\Delta Oc/\Delta Oc}$ mice are an example of an in vivo phenomenon regulating osteoblast differentiation by osteoclasts during bone remodeling. These findings suggest a new paradigm: BMPR1A signaling in osteoclasts mediates coupling of bone resorption and formation.

It remains necessary to define how BMP signals in osteoclasts regulate the bone-forming activities of osteoblasts. Several molecules, including TGF-β and ephrinB2, are considered to be coupling factors that regulate osteoblast differentiation.[3–6] These molecules are released from bone matrix after osteoclastic resorption, activated by osteoclasts, or produced by osteoclasts. Further studies are needed to determine whether these molecules mediate BMPR1A-induced coupling from osteoclasts to osteoblasts. Taken together with the previous findings that BMP signals in osteoblasts regulate osteoclastic bone resorption,[20] this study suggests that BMPs are not only stimulators of osteoblast differentiation but also are regulators of reciprocal interactions between osteoblasts and osteoclasts to fine-tuning bone mass during bone remodeling. Our results indicate that BMPs regulate bone formation and maintenance in a more complex manner than previously thought.

## Disclosures

All the authors state that they have no conflicts of interest.

## Acknowledgments

This study was supported in part by Scientific Research Grant Numbers 20791033, 18390415, 19659378, and 21390421 from MEXT, JST, and CREST to NT and DE020843 to YM.

Authors' roles: MO and NT conceived the project. MO performed most of experiments. JM generated Col1a1-Cre mice. DI performed some experiments. YI and SK prepared *Ctsk-Cre* mice. NK and YM prepared *Bmpr1a* flox mice. MO, YI, NK, YM, HY, and NT discussed results. MO, YM, and NT wrote the manuscript.

## References

1. Olsen BR, Reginato AM, Wang W. Bone development. Annu Rev Cell Dev Biol. 2000;16:191–220.
2. Boyle WJ, Simonet WS, Lacey DL. Osteoclast differentiation and activation. Nature. 2003;423:337–42.
3. Pfeilschifter J, Mundy GR. Modulation of type β transforming growth factor activity in bone cultures by osteotropic hormones. Proc Natl Acad Sci USA. 1987;84:2024–8.
4. Tang Y, Wu X, Lei W, Pang L, Wan C, Shi Z, Zhao L, Nagy TR, Peng X, Hu J, Feng X, Van Hul W, Wan M, Cao X. TGF-β1-induced migration of bone mesenchymal stem cells couples bone resorption with formation. Nat Med. 2009;15:757–65.
5. Zhao C, Irie N, Takada Y, Shimoda K, Miyamoto T, Nishiwaki T, Suda T, Matsuo K. Bidirectional ephrinB2-EphB4 signaling controls bone homeostasis. Cell Metab. 2006;4:111–21.
6. Matsuo K, Irie N. Osteoclast-osteoblast communication. Arch Biochem Biophys. 2008;473:201–9.
7. Urist MR. Bone: formation by autoinduction. Science. 1965;150:893–9.
8. Wozney JM, Rosen V, Celeste AJ, Mitsock LM, Whitters MJ, Kriz RW, Hewick RM, Wang EA. Novel regulators of bone formation: molecular clones and activities. Science. 1988;242:1528–34.
9. Shi Y, Massague J. Mechanisms of TGF-beta signaling from cell membrane to the nucleus. Cell. 2003;113:685–700.
10. Zhao M, Harris SE, Horn D, Geng Z, Nishimura R, Mundy GR, Chen D. Bone morphogenetic protein receptor signaling is necessary for normal murine postnatal bone formation. J Cell Biol. 2002;157:1049–60.
11. Mishina Y, Starbuck MW, Gentile MA, Fukuda T, Kasparcova V, Seedor JG, Hanks MC, Amling M, Pinero GJ, Harada S, Behringer RR. Bone morphogenetic protein type IA receptor signaling regulates postnatal osteoblast function and bone remodeling. J Biol Chem. 2004;279:27560–6.
12. Okamoto M, Murai J, Yoshikawa H, Tsumaki N. Bone morphogenetic proteins in bone stimulate osteoclasts and osteoblasts during bone development. J Bone Miner Res. 2006;21:1022–33.
13. Sotillo Rodriguez JE, Mansky KC, Jensen ED, Carlson AE, Schwarz T, Pham L, MacKenzie B, Prasad H, Rohrer MD, Petryk A, Gopalakrishnan R. Enhanced osteoclastogenesis causes osteopenia in twisted gastrulation-deficient mice through increased BMP signaling. J Bone Miner Res. 2009;24:1917–26.
14. Itoh K, Udagawa N, Katagiri T, Iemura S, Ueno N, Yasuda H, Higashio K, Quinn JM, Gillespie MT, Martin TJ, Suda T, Takahashi N. Bone morphogenetic protein 2 stimulates osteoclast differentiation and survival supported by receptor activator of nuclear factor-kappaB ligand. Endocrinology. 2001;142:3656–62.
15. Kanatani M, Sugimoto T, Kaji H, Kobayashi T, Nishiyama K, Fukase M, Kumegawa M, Chihara K. Stimulatory effect of bone morphogenetic protein-2 on osteoclast-like cell formation and bone-resorbing activity. J Bone Miner Res. 1995;10:1681–90.
16. Kaneko H, Arakawa T, Mano H, Kaneda T, Ogasawara A, Nakagawa M, Toyama Y, Yabe Y, Kumegawa M, Hakeda Y. Direct stimulation of osteoclastic bone resorption by bone morphogenetic protein (BMP)-2 and expression of BMP receptors in mature osteoclasts. Bone. 2000;27:479–86.
17. Giannoudis PV, Kanakaris NK, Einhorn TA. Interaction of bone morphogenetic proteins with cells of the osteoclast lineage: review of the existing evidence. Osteoporos Int. 2007;18:1565–81.
18. Wildemann B, Kadow-Romacker A, Lubberstedt M, Raschke M, Haas NP, Schmidmaier G. Differences in the fusion and resorption activity of human osteoclasts after stimulation with different growth factors released from a polylactide carrier. Calcif Tissue Int. 2005;76:50–5.
19. Jensen ED, Pham L, Billington CJ Jr, Espe K, Carlson AE, Westendorf JJ, Petryk A, Gopalakrishnan R, Mansky K. Bone morphogenic protein 2 directly enhances differentiation of murine osteoclast precursors. J Cell Biochem. 2010;109:672–82.
20. Kamiya N, Ye L, Kobayashi T, Lucas DJ, Mochida Y, Yamauchi M, Kronenberg HM, Feng JQ, Mishina Y. Disruption of BMP signaling in osteoblasts through type IA receptor (BMPRIA) increases bone mass. J Bone Miner Res. 2008;23:2007–17.
21. Kamiya N, Ye L, Kobayashi T, Mochida Y, Yamauchi M, Kronenberg HM, Feng JQ, Mishina Y. BMP signaling negatively regulates bone mass through sclerostin by inhibiting the canonical Wnt pathway. Development. 2008;135:3801–11.
22. Mishina Y, Hanks MC, Miura S, Tallquist MD, Behringer RR. Generation of Bmpr/Alk3 conditional knockout mice. Genesis. 2002;32:69–72.
23. Nakamura T, Imai Y, Matsumoto T, Sato S, Takeuchi K, Igarashi K, Harada Y, Azuma Y, Krust A, Yamamoto Y, Nishina H, Takeda S, Takayanagi H, Metzger D, Kanno J, Takaoka K, Martin TJ, Chambon P, Kato S. Estrogen prevents bone loss via estrogen receptor alpha and induction of Fas ligand in osteoclasts. Cell. 2007;130:811–23.
24. Iwai T, Murai J, Yoshikawa H, Tsumaki N. Smad7 Inhibits chondrocyte differentiation at multiple steps during endochondral bone formation and down-regulates p38 MAPK pathways. J Biol Chem. 2008;283:27154–64.
25. Koga T, Inui M, Inoue K, Kim S, Suematsu A, Kobayashi E, Iwata T, Ohnishi H, Matozaki T, Kodama T, Taniguchi T, Takayanagi H, Takai T. Costimulatory signals mediated by the ITAM motif cooperate with RANKL for bone homeostasis. Nature. 2004;428:758–63.
26. Hanley T, Merlie JP. Transgene detection in unpurified mouse tail DNA by polymerase chain reaction. Biotechniques. 1991;10:56.
27. Quinn JM, Itoh K, Udagawa N, Hausler K, Yasuda H, Shima N, Mizuno A, Higashio K, Takahashi N, Suda T, Martin TJ, Gillespie MT. Transforming growth factor beta affects osteoclast differentiation via direct and indirect actions. J Bone Miner Res. 2001;16:1787–94.
28. Miyazaki T, Katagiri H, Kanegae Y, Takayanagi H, Sawada Y, Yamamoto A, Pando MP, Asano T, Verma IM, Oda H, Nakamura K, Tanaka S. Reciprocal role of ERK and NF-kappaB pathways in survival and activation of osteoclasts. J Cell Biol. 2000;148:333–42.
29. Takahashi N, Udagawa N, Akatsu T, Tanaka H, Isogai Y, Suda T. Deficiency of osteoclasts in osteopetrotic mice is due to a defect in the local microenvironment provided by osteoblastic cells. Endocrinology. 1991;128:1792–6.
30. Suda T, Jimi E, Nakamura I, Takahashi N. Role of 1 alpha,25-dihydroxyvitamin D3 in osteoclast differentiation and function. Methods Enzymol. 1997;282:223–35.
31. Horiki M, Imamura T, Okamoto M, Hayashi M, Murai J, Myoui A, Ochi T, Miyazono K, Yoshikawa H, Tsumaki N. Smad6/Smurf1 overexpression in cartilage delays chondrocyte hypertrophy and causes dwarfism with osteopenia. J Cell Biol. 2004;165:433–45.
32. Tsumaki N, Liu Y, Yamada Y, Krebsbach P. Enhancer analysis of the alpha 1(II) and alpha 2(XI) collagen genes in transfected chondrocytes and transgenic mice. Methods Mol Biol. 2000;139:187–95.

33. Saftig P, Hunziker E, Wehmeyer O, Jones S, Boyde A, Rommerskirch W, Moritz JD, Schu P, von Figura K. Impaired osteoclastic bone resorption leads to osteopetrosis in cathepsin-K-deficient mice. Proc Natl Acad Sci U S A. 1998;95:13453–8.
34. Lotinun S, Evans GL, Bronk JT, Bolander ME, Wronski TJ, Ritman EL, Turner RT. Continuous parathyroid hormone induces cortical porosity in the rat: effects on bone turnover and mechanical properties. J Bone Miner Res. 2004;19:1165–71.
35. Rhee Y, Allen MR, Condon K, Lezcano V, Ronda AC, Galli C, Olivos N, Passeri G, O'Brien CA, Bivi N, Plotkin LI, Bellido T. PTH receptor signaling in osteocytes governs periosteal bone formation and intra-cortical remodeling. J Bone Miner Res. DOI 10.1002/jbmr.304.
36. Bellido T, Ali AA, Gubrij I, Plotkin LI, Fu Q, O'Brien CA, Manolagas SC, Jilka RL. Chronic elevation of parathyroid hormone in mice reduces expression of sclerostin by osteocytes: a novel mechanism for hormonal control of osteoblastogenesis. Endocrinology. 2005;146:4577–83.
37. Rossert J, Eberspaecher H, de Crombrugghe B. Separate cis-acting DNA elements of the mouse pro-alpha 1(I) collagen promoter direct expression of reporter genes to different type I collagen-producing cells in transgenic mice. J Cell Biol. 1995;129:1421–32.
38. Sakai K, Miyazaki J. A transgenic mouse line that retains Cre recombinase activity in mature oocytes irrespective of the cre transgene transmission. Biochem Biophys Res Commun. 1997;237:318–24.
39. Kamiya N, Kobayashi T, Mochida Y, Yu PB, Yamauchi M, Kronenberg HM, Mishina Y. Wnt inhibitors Dkk1 and Sost are downstream targets of BMP signaling through the type IA receptor (BMPRIA) in osteoblasts. J Bone Miner Res. 25:200–10.